Astron. Astrophys. 320, 945–956 (1997)

ASTRONOMY
AND
ASTROPHYSICS

Loop modeling of coronal X-ray spectra

III. Fitting loop spectra with one- and two-component thermal models

A. Ciaravella[⋆], **A. Maggio, and G. Peres**

Istituto ed Osservatorio Astronomico, Piazza del Parlamento 1, 90134 Palermo, Italy
(amaggio@oapa.astropa.unipa.it, gperes@oapa.astropa.unipa.it)

Received 11 June 1996 / Accepted 23 September 1996

Abstract. In this work we study coronal loops vs. one- and two-component thermal models, the first being the physically realistic description of the X-ray emitting, magnetically-confined solar corona, the others the standard analysis tool of X-ray spectra from stellar coronae. The scope of this work is to compare directly these two paradigms of coronal physics, also to find a possible relation between the loop characteristics and the findings of the thermal components fitting. We simulate observations of coronal spectra using a static loop model, including the effects of stellar gravity and of possible non-uniform loop cross-section. We evaluate the one- and two-temperature fitting results through extensive simulations, varying the loop parameters, the photon counting statistics, and considering two instruments: the ROSAT/PSPC and the ASCA/SIS. We find that one-temperature models do not fit adequately loop spectra with 10^3 total counts or more, for any of the cases explored. Two-temperature models provide a good fit to single loop spectra in many of the cases explored, with the implication that the two temperatures found when fitting real observations may not necessarily indicate the presence of two classes of dominating loops in the observed corona, but rather may be explained with only one class of loops, as long as the ratio of the emission measures of the hot vs. cool component is larger than unity. The goodness of the fit becomes worse with increasing photon statistics and/or resolving power, especially for loops with relatively intense plasma pressure ($p_0 > 10$ dyn cm^{-2}) and as high as the pressure scale height. In such cases the two-temperature fitting and the loop modeling are therefore not equivalent, implying that, for such kind of observations, detailed loop fitting should be attempted. We comment on our findings and draw possible guidelines to interpret observations.

Key words: stars: coronae – stars: late-type; plasmas – X-rays: stars

Send offprint requests to: A. Maggio

⋆ Currently at the SOHO/UVCS Experiment Operation Facility, Goddard Space Flight Center, Washinghton D.C., USA

1. Introduction

X-ray astronomy provides fundamental clues on the physics of stellar activity (Rosner et al. 1985). The overall scenario of X-ray stellar physics is quite rich and detailed, but the analysis of individual stars' coronae is not equally detailed, while we know of the very complex morphology of the Sun's corona. By the same token, the physical interpretation of coronal observations is made differently for stars and for the Sun.

In particular, X-ray spectra of stellar coronae have been traditionally fitted with thermal models consisting of one or, at most, two plasma components at different temperatures, a method that we call in the following 1-T or 2-T fitting (Vaiana et al., 1981, Schmitt et al. 1990). This approach has been initially valuable in proving the thermal (i.e. coronal) nature of X-ray stellar emission and has given estimates of a somehow average temperature of the emitting coronal plasma; however, it yields a very coarse picture of a X-ray corona. Instead, from observations of the Sun, the best known example and a valid template for a coronal source, one is led to believe that stellar coronae are entirely made of magnetic loops. Indeed, the X-ray emitting solar corona has a very complex morphology and thermal structure, being entirely composed by a multitude of magnetic arches confining hot plasma; the plasma in each arch is, in practice, energetically and dynamically independent from that of the other arches, and each arch can then be considered as an independent unit of solar corona, a mini- corona by itself (Rosner et al. 1978). Magnetic loops are considered the building blocks of the corona and they have become, since Skylab, the key paradigm to understand and describe solar X-ray activity.

The data on stellar coronae do not grant to achieve an equally detailed picture but certainly the coronal loop should be taken as the key feature to understand the relevant physics, analogously to what happened for the solar corona. In this respect, there have been some attempts to fit the stellar coronal emission in terms of a coronal loop spectrum (Schmitt et al. 1985; Giampapa et al. 1985; Landini et al. 1985; Stern et al. 1986; Schrijver et al. 1989; Ottman 1993) but the picture is far from being complete.

On the other hand, the 1-T and 2-T fittings, in spite of all their limitations, are still the workhorse for the data analysis of stellar X- ray spectra, and they may work better than loop modeling for low counts spectra. Therefore, it may be worth trying to understand which features of loop physics can be identified with 1-T and 2-T fittings, and where they fail to give accurate information on the coronal loops. Some authors have already tried to interpret the results of two-temperature fits in terms of loop structures: it has been sometimes assumed that each of the temperatures derived with thermal fittings is that of one kind of dominating loop structures[1] (Schrijver et al. 1989; Lemen et al. 1989; Giampapa et al. 1996). Such an interpretation, however, is not sufficiently well based, has to be taken with a bit of caution, and can be justified only as a first attempt to derive a physically meaningful picture of coronae with data of low spectral resolution or low signal-to-noise ratio.

This paper is part of a project dedicated to study stellar coronal loop structures, their spectra and their application to the interpretation of observed X-ray coronal data. Ciaravella et al. (1996) (henceforth Paper I) have revisited some characteristics of coronal loops, such as the thermal conduction regime and the widening loop cross-section, and studied their influence on the temperature and density stratification inside the loop, and ultimately on the spectrum emitted by the whole loop, in order to evaluate the observability of such characteristics in the spectra obtained with X-ray telescopes such as ROSAT, ASCA and XMM. Paper II (Maggio and Peres 1996) was dedicated to ascertain the diagnostic power of fitting loop spectra to observations of Einstein/IPC, ROSAT/PSPC and ASCA/SIS.

This work is dedicated to compare loop modeling of coronal X-ray observations with 1-T and 2-T fittings of the same data, in order to understand, for instance, how the temperature derived with the thermal fitting compares with the maximum loop temperature, whether or not - as sometimes assumed - each of the two temperatures fitted corresponds to a class of dominating loop structures, and the extent to which instrumental characteristics and loop physics can limit our task of deriving coronal conditions. To this end we use static loop models to simulate a steady corona dominated by one kind of loops, and we generate realistic photon counts spectra collected with the ROSAT/PSPC and ASCA/SIS; we then make a 1-T and 2-T fit of such synthesized spectra. We use the ASAP environment (Maggio et al. 1994a) to synthesize the spectrum and to present and interpret the results of our analysis, and the XSPEC environment to perform the fittings.

In the present paper, Sect. 2 briefly describes the loop modelling and spectrum synthesis procedures, Sect. 3 is devoted to presenting the results, and in Sect. 4 we discuss our findings and draw our conclusions.

[1] It is worth noting that the identification, sometimes made of such temperature with the *maximum loop temperature* is incorrect since it does not take into account the weighting and averaging effect of observing a plasma distribution through the spectral response of an instrument, leading to an effective temperature certainly lower than the maximum one.

Table 1. Loop parameters

ID	L (10^{10} cm)	p_0 (dyn cm^{-2})	$T_{\max}$ (10^6 K)	$H/s_{\rm p}$	PSPC Rate[1] (cnt s^{-1})	SIS Rate[1] (cnt s^{-1})
α	0.56	1.78	3.0	0.2	0.7	0.04
β	1.00	5.62	5.4	0.2	4.1	0.6
γ	1.00	10.0	6.6	0.2	9.4	1.7
δ	1.78	17.8	9.6	0.2	23.1	5.1
ϵ	3.16	100.	20.	0.2	197.6	51.1
ζ	5.62	1.78	6.4	1.0	0.9	0.1
η	10.0	5.62	11.3	1.0	5.4	1.1
θ	17.8	10.0	16.4	1.0	12.1	2.6
ι	17.8	17.8	20.	1.0	26.1	6.2
κ	31.6	100.	42.6	1.0	251.4	71.7

[1] Count rates computed assuming that the emission originates from a sun-like star ($R_* = 7 \times 10^{10}$ cm), with surface filling factor $f = 1$, and distance $D = 10$ pc from the Sun.

2. Loop models and spectra

We assume that the coronal emission entirely originates from plasma magnetically confined inside steady loop structures of toroidal geometry and mirror symmetric with respect to their apex. We consider loops either with a constant loop cross section or with a cross section widening from the base to the apex of the loop (cf. Paper I). Since here we are interested in the coronal stellar emission outside evident flares, and therefore to loop structures that remain unchanged over time lapses much longer than the characteristic dynamic and thermodynamic times of plasma, we make the hypothesis of hydrostatic conditions. Our loop plasma model (Serio et al. 1981; cf. also Paper I) describes the plasma as a fluid with a steady energy balance among uniform heating input, heat conduction and optically thin radiative losses. Each loop configuration, for a prescribed law of loop widening, is uniquely characterized by the loop length and the plasma pressure at the base of the transition region. For further details and for some applications to the interpretation of X-ray stellar observations, we refer to Paper I and Paper II.

In this work, since we are just interested to the comparison of the loop model with 1-T and 2-T fittings, we have chosen to refer to a representative solar-like star ($R_* = R_\odot$, $g_* = g_\odot$). We have computed models of loop structures over ranges of loop physical parameters wide enough to cover a large set of conditions of solar-type stellar coronae. In particular, the base pressure, p_0, and the loop semi-length, L, may assume values in the range $[0.03 \div 300]$ dyne cm^{-2} and $[3 \times 10^8 \div 1 \times 10^{12}]$ cm, respectively. The corresponding range of maximum temperature in the loop models is $[2.5 \times 10^5 \div 9.5 \times 10^7]$ K.

On the basis of the density and temperature stratification inside the loop and using the Raymond's (1989) emissivity func-

tion for optically thin plasmas, we compute the spectrum for each loop model as:

$$I(j) = \frac{2\pi {R_\star}^2}{4\pi D^2} f \int_0^L n_{\rm p}(s) n_{\rm e}(s) G(T(s), j)\ S(s)\ {\rm d}s \qquad (1)$$

(counts s^{-1})

where $R_\star$ and D are the radius of the star and its distance from the Sun, respectively, f the surface filling factor, i.e. the fraction of star's surface covered by the loops footpoints, L is the loop semilength, n_e and n_p are the electron and proton densities, T the temperature along the loop, S the loop cross section area normalized to the base area, and s the curvilinear coordinate along the loop. $G(T(s), j)$ is the plasma emissivity convolved through the instrument effective area, $A(E)$, and the energy response matrix, $M(j, E)$, and it is given by:

$$G(T(s), j) \ = \ \int \ \frac{P(T, E)}{E} A(E) M(j, E) {\rm d}E \qquad (2)$$

(counts s^{-1} cm^5)

where j is an index running over the instrument energy channels, $P(T, E)$ is the emissivity function for an optically thin plasma, and E the photon energy. Here we simulate observations with two different instruments, widely used to observe coronae, ROSAT/PSPC and ASCA/SIS. For ROSAT/PSPC we synthesize the model spectra adopting the 34 channel scheme used by the standard ROSAT data processing (SASS), while for ASCA/SIS we produce spectra with the standard 512 energy bins. We also consider the effect of Poisson statistical noise on the number of photons in each energy bin of the detector.

With the 1-T and the 2-T fitting to the synthesized spectra we obtain, for the 1-T, the plasma temperature and the normalization $EM/4\pi D^2$ (where EM is the emission measure), while for the 2-T fitting, the two temperatures, T_1 and T_2 (with $T_2 > T_1$), and the two corresponding normalizations, from which the ratio EM_2/EM_1 is computed.

The simulation, for each loop structure, consists of at least 200 realizations (i.e. randomizations of the same parent spectrum) for which a best-fit 1-T or 2-T model is searched on the basis of the χ^2 statistics. In order to test for the goodness of the fit, we have adopted a χ^2 threshold corresponding to the 90% confidence level appropriate for the number of degrees of freedom (DOF) of each simulation. Since it is well known (Eadie et al. 1982) that energy bins with few counts do not contribute properly to the χ^2, we have adjusted the nominal number of DOF, for each simulation, to take into account this effect, as explained in detail in the Appendix. These corrections make sure that the χ^2 values resulting from the fitting of simulated spectra are distributed according to the χ^2 distribution (c.f. also Maggio et al. 1995).

3. Results

In the following we focus our attention on the results about a subset of loop structures, illustrative of the whole set that we have considered. In Table 1, for each loop model of this subset, we give the loop semilength L, the base pressure p_0, the maximum temperature $T_{\rm max}$ (located at the loop's apex), $H/s_{\rm p}$, i.e. the ratio between the height of the loop apex above the star surface and the pressure scale height (in Paper II we have shown the importance of $H/s_{\rm p}$ in characterizing coronal loop spectra), the PSPC count rate and the SIS count rate assuming a sun-like star with unity surface filling factor and located 10 pc away from the Sun. In particular, we have selected two groups of loop models, already considered in Paper II: the first group comprises five loops with increasing plasma base pressure and semi-length chosen so to obtain $H/s_{\rm p} \approx 0.2$; in the second group, the five loops have the same p_0 as in the first group but $H/s_{\rm p} \approx 1$. It is worth mentioning that loop atmospheres with pressure lower than the ones reported in Table 1 require unrealistic values either of observing time, or of surface filling factor or of star's distance from the Sun, or combinations thereof, in order to achieve the number of counts assumed in our study.

In order to illustrate how the counting statistics affects our findings, we have simulated observations, for different combinations of surface filling factor, distance and observing time so

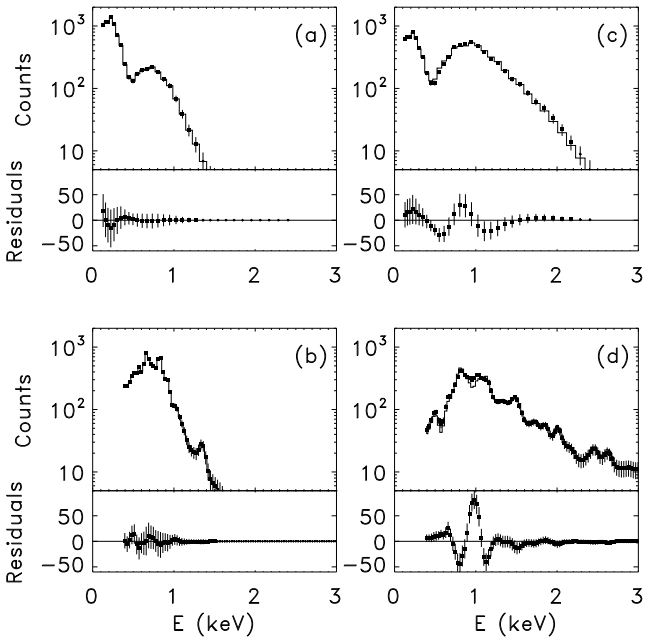

Fig. 1a–d. Sample loop spectra, best-fit 2-T models, and fit residuals. **a** Simulated spectrum for a loop with p_0 = 1.8 dyne cm^{-2} and L = 5.6 $\times$ 10^9 cm (case α in Table 1), assuming 10^4 total counts collected with the ROSAT/PSPC. The 2-T model provides an acceptable fit to this spectrum yielding $\chi^2_{\rm red}$ = 1.1 with 26 d.o.f. **b** Same loop spectrum as in **a**, but folded with the ASCA/SIS spectral response ($\chi^2_{\rm red}$ = 1.2, d.o.f. 51). **c** ROSAT/PSPC spectrum and **d** ASCA/SIS spectrum for a loop with p_0 = 100 dyne cm^{-2} and L = 3.2 $\times$ 10^{11} cm (case κ in Table 1), with the same number of total counts as in **a** and **b**. For this spectrum the 2-T model does not yield an acceptable fit ($\chi^2_{\rm red}$ = 2.0 with 32 d.o.f. for the PSPC spectrum; $\chi^2_{\rm red}$ = 1.5 with 207 d.o.f. for the SIS spectrum; note that the number of d.o.f. is larger than in **a** and **b** because fewer "empty" energy bins were discarded)

as to obtain either 10^3 or 10^4 total counts with ROSAT/PSPC, and either 10^4 or 10^5 counts with ASCA/SIS, for each coronal model. These count figures are representative, respectively, of typical good stellar observation and of the much less numerous observations yielding very high signal-to-noise ratio spectra.

Before presenting the results of the simulations performed, we find it useful to show here four examples and some of the details common to the procedure we have followed in each case, so to clarify the following results shown in a schematic form.

Fig. 1 shows some examples of simulated loop spectra, 2-T best-fit models, and fit residuals. For ease of comparison, we have selected two loop spectra with characteristics at the extremes of the set considered (α and κ in Table 1), folded with the ROSAT/PSPC spectral response (upper panels) and with the ASCA/SIS spectral response (lower panels). The total number of counts is 10^4 in all the cases shown. As better explained below, the spectrum of case α can be well approximated by a 2-T model, while the other cannot, for both the instruments here considered.

The scatter plots in Fig. 2 show examples of the distributions of the best-fit 2-T model parameters, namely the temperatures and the ratio of the emission measures, for 200 realizations of the input loop spectrum identified as α in Table 1, with independent Poisson noise included. From this kind of distributions, we derive the median value and the central 68% interquartile range for each simulation. In the following we adopt the latter figure as an estimate of the uncertainty at the 68% confidence level that would be derived from the analysis of real data.

Figs. 3 to 6 show, in a schematic form, the results of 1-T and 2-T fittings of the simulated spectra, assuming stellar coronal sources entirely composed of each one of the loop kinds reported in Table 1.

3.1. ROSAT/PSPC simulations

Fig. 3 pertains to ROSAT/PSPC spectra with 10^3 counts, and shows results of 1-T fittings (panel a), in the form of box-plots of the fitted temperature values, and of 2-T fittings (panels b and c), in the form of box-plots of T_1 and T_2, and of the ratio of the emission measures EM_2/EM_1; finally, panel d shows the values of reduced χ^2 (in the following $\chi^2_{\rm red}$) of the best-fit models for the 1-T and 2-T fittings, along with the $\chi^2_{\rm red}$ value at the 90% confidence level, i.e. the threshold for rejection of the model hypothesis, computed for the appropriate number of degrees of freedom (see Appendix). Whenever the values are beyond the upper boundary of the graph, they are marked with an arrow along with the relevant value. More in particular, the central horizontal line in each box marks the median value of the distribution, and the upper and lower edges mark the boundary of the 68% interquartile range. For ease of comparison, in panels a and b the diamonds indicate the value of the peak loop temperature.

Panels a to d illustrate the results for loops with $H/s_{\rm p}$ = 0.2, panels e to h illustrate the analogous results for loops with $H/s_{\rm p}$ = 1. In the latter cases, the fitted temperatures are usually slightly higher than the corresponding cases with $H/s_{\rm p}$ = 0.2,

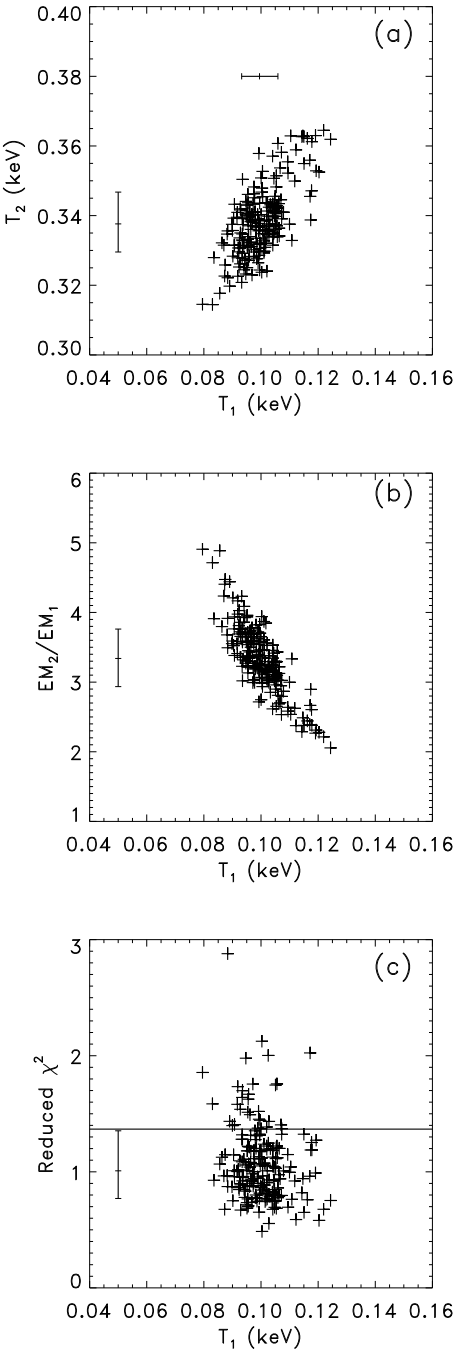

Fig. 2a–c. Scatter plots of best-fit 2-T model parameters and $\chi^2_{\rm red}$ values for 200 realizations of the loop spectrum in Fig. 1a. The marks on the horizontal and vertical error bars in each panel indicate the median value of the distributions and the 68% interquartile range. **a** Scatter plot of the two fitted temperatures, T_1 and T_2. **b** Scatter plot of the fitted emission measure ratio, EM_2/EM_1 vs. T_1. **c** Scatter plot of $\chi^2_{\rm red}$ vs. T_1. The solid line indicates the fit acceptance threshold at the 90% confidence level

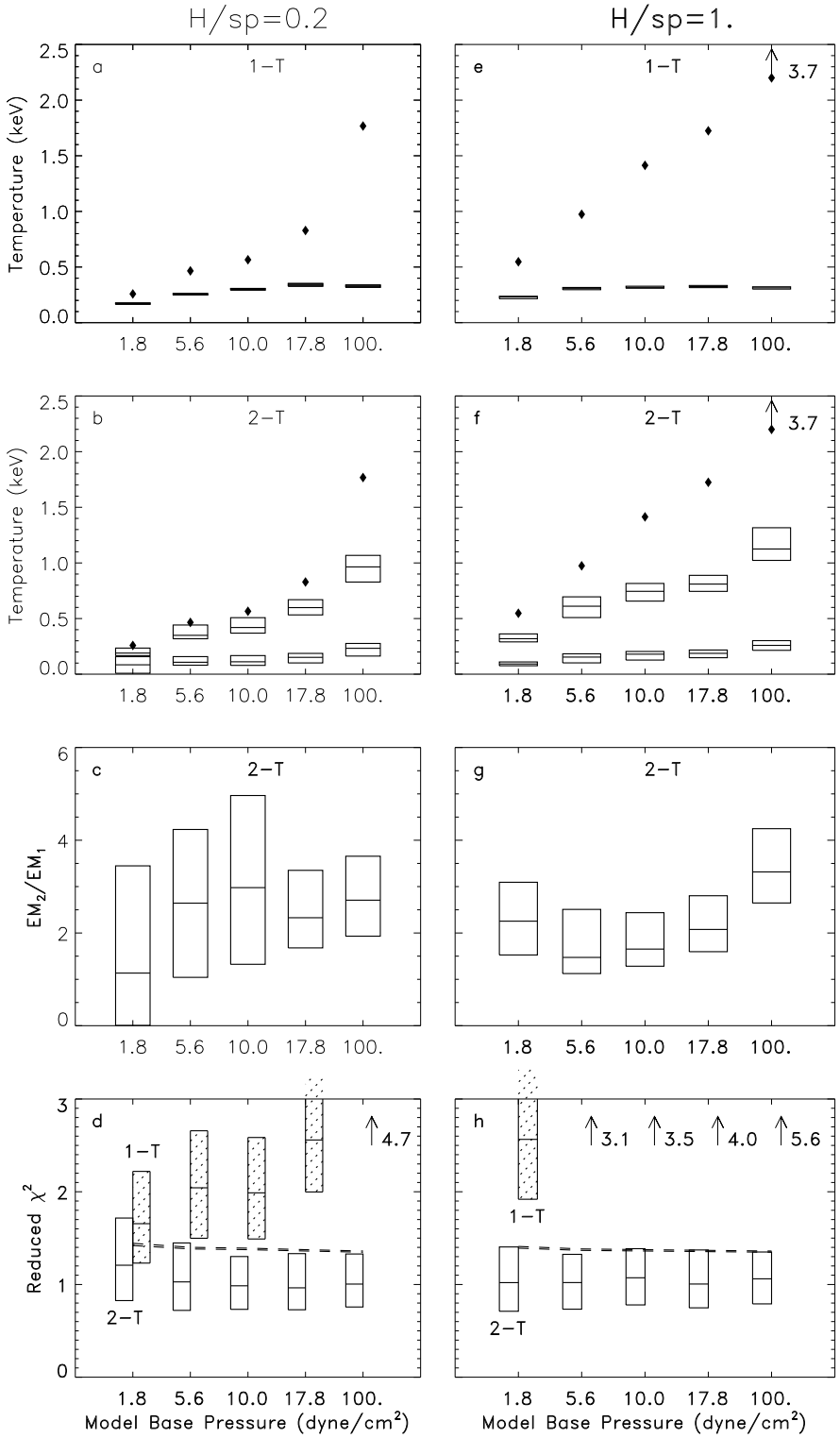

Fig. 3a–h. Results of simulations of ROSAT/PSPC spectra with 10^3 total counts. All the panels on the left refer to loops with $H/s_p \approx 0.2$, those on the right to loops with $H/s_p \approx 1$. The four panels in each column show, from top to bottom, boxplots of the fitted temperature for the 1-T model (**a,e**), the two temperatures (**b,f**) and the emission measure ratio (**c,g**) for the 2-T model, the χ^2_{red} values (**d,h**) for both the 1-T and the 2-T models. In each box, the central horizontal line marks the median value of the distribution, while the upper and lower edges mark the central 68% interquartile range. Whenever the median values are beyond the upper boundary of the graph, they are shown along with an arrow. In the panels (a,e) and (b,f) the solid diamonds indicate the value of the loop plasma maximum temperature. In the panels (d,h) the hatched boxes refer to the fitting results with the 1-T model, and the empty boxes to those with the 2-T model. The dashed horizontal line indicates the χ^2_{red} values at the 90% confidence level, with the number of degrees of freedom appropriate to each simulated spectrum (see Appendix); since the number of d.o.f. differs slightly from one case to another, the line in panels (d,h) is inclined. Note that the 90% confidence levels are drawn for both the 1-T and the 2-T fittings, but they are practically indistinguishable

especially for the hot component of the 2-T fitting model (but also the maximum loop temperature is higher); the ratio of the emission measures (panel g) is better defined, i.e. the 68% limits in each boxplot are closer to the fitted values with respect to the case with $H/s_p = 0.2$. The 2-T fittings for $H/s_p = 1$ are equally as good as for the $H/s_p = 0.2$ cases, while the 1-T model yields even worse fittings, as indicated by the χ^2_{red} values (panel h).

From these results it is evident that the 2-T fitting of coronal spectra with 10^3 counts in the ROSAT/PSPC invariably gives more acceptable results, i.e. lower χ^2_{red} values, than those obtained with 1-T fittings. The latter give a median χ^2_{red} value higher than the acceptance threshold, for all coronal loop models in Fig. 3; the χ^2_{red} values increase with the maximum temperature of the coronal loop and are even higher for $H/s_p = 1$.

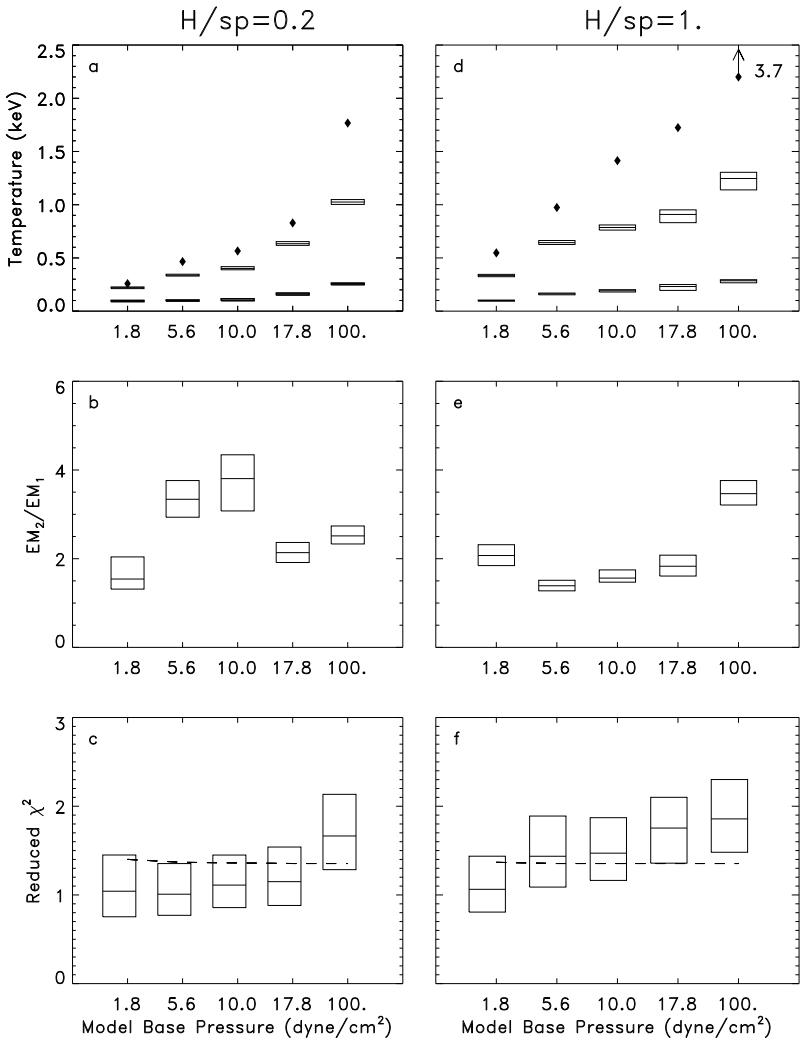

Fig. 4a–f. Similar to Fig. 3, but for ROSAT/PSPC spectra with 10^4 total counts. Only results relative to the fittings with the 2-T model are shown. **a,d** boxplots of the fitted temperatures; **b,e** boxplots of the emission measure ratio; **c,f** boxplots of $\chi^2_{\rm red}$

The 2-T fittings are characterized by a relatively large indetermination in the ratio EM_2/EM_1 especially for the coronal loops with $H/s_{\rm p}$ = 0.2 and with the lowest values of plasma pressure. It is worth noting that the median ratio EM_2/EM_1 is invariably between 1 and 4; we will discuss the implications of this result in more detail in the next section.

Fig. 4 is analogous to Fig. 3, but shows the results of simulating observations yielding 10^4 counts. The 1-T fitting results have been omitted from Fig. 4 to improve readability, since they are of quality comparable to those in Fig. 3; indeed, they give values of $\chi^2_{\rm red}$ always higher than the corresponding simulations with 10^3 counts, and well above the 90% confidence level already for coronal loops with the lowest plasma pressure. These simulations indicate that the 1-T model is always inadequate to fit coronal loop spectra with 10^4 counts in the ROSAT/PSPC. This finding is interestingly analogous to results already obtained in the spectral analysis of real stellar observations, as we will further discuss in the next section.

The 2-T fitting gives, again, results significantly better than the 1-T fitting, and the corresponding parameter EM_2/EM_1 is well determined (panel c and f of Fig. 4). It is worth noting, however, that the loops with the highest pressure (ϵ, ι, κ) tend to yield unacceptable $\chi^2_{\rm red}$ values and therefore, as the counts statistics increases, also the two-temperature model becomes inappropriate to fit the loop spectra.

Finally, we note that the loop peak temperature is always higher than the temperature of the hot component in the 2-T model, and the separation between them increases with increasing base pressure.

3.2. ASCA/SIS simulations

We have performed analogous simulations for the ASCA/SIS instrument, for 10^4 and 10^5 total collected counts, so as to obtain count statistics *per energy resolution channel* similar to that obtained for ROSAT/PSPC in the cases previously discussed, given the larger number of channels in the SIS (512 channels) with respect to the PSPC (34 channels). The spectral pass-band of the two instruments is, however, significantly different and an accurate direct comparison of the relevant cases is not possible. Fig. 5 is analogous to Fig. 3, and shows the results of our simulations for 10^4 total counts. The results for the simulations with 10^5 total counts are not shown, but we report on them below.

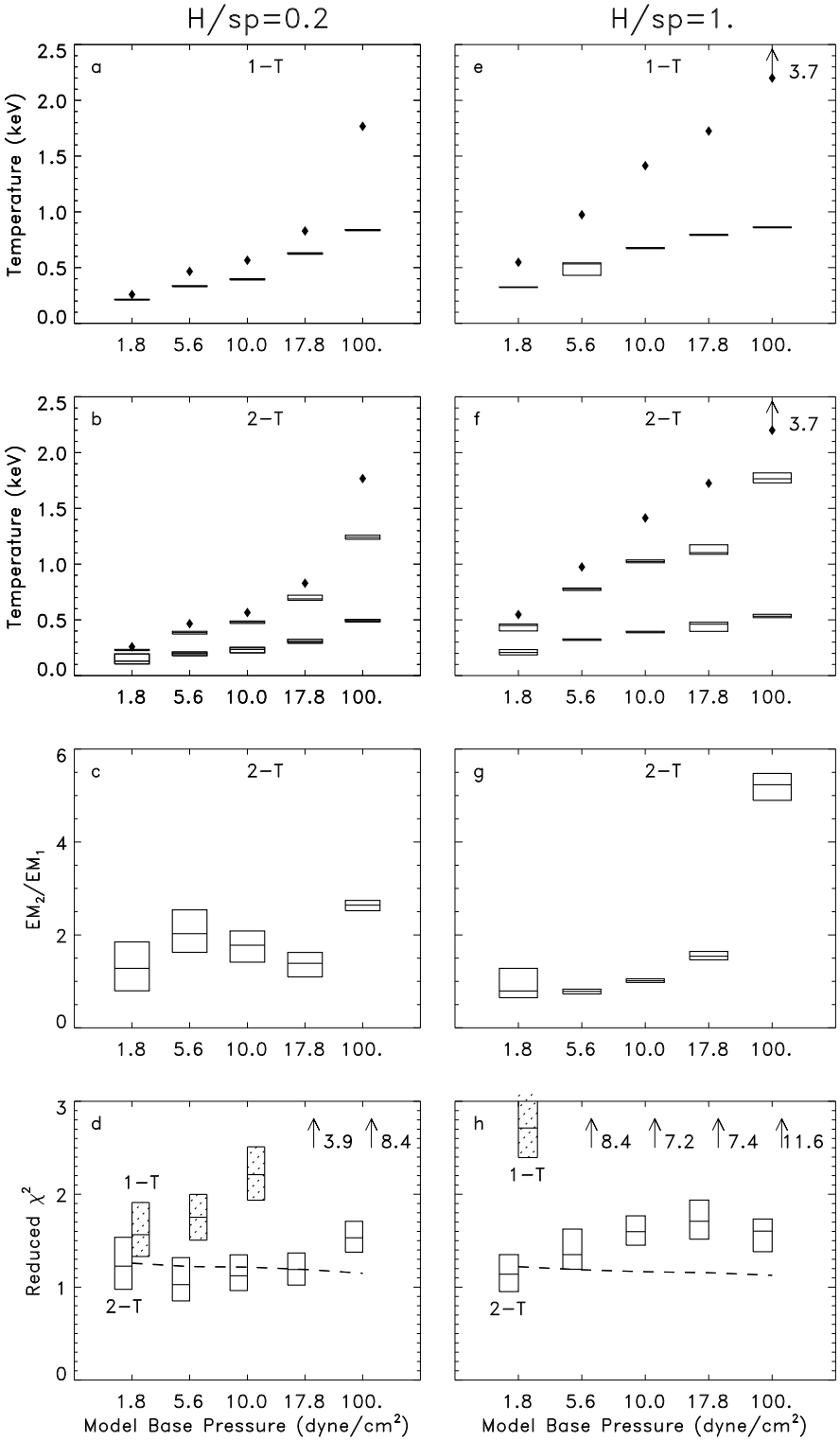

Fig. 5a–h. Simulations of ASCA/SIS loop spectra with 10^4 total collected counts, and their fitting results. The arrangement of panels and symbols is the same as in Fig. 3

Also for the ASCA/SIS the 1-T fitting yields worse results than the corresponding 2-T fittings, as illustrated by the panel d of Fig. 5. The 2-T fittings however tend to yield $\chi^2_{\rm red}$ values worse than the corresponding cases analyzed for ROSAT/PSPC, especially for the loops with peak plasma temperature above 1 keV (ϵ and η through κ), while the EM_2/EM_1 ratio is instead more sharply determined, as shown by the size of the boxes in the panel c. More specifically, already the case with the highest plasma pressure and $H/s_{\rm p} = 0.2$ in Fig. 5, and all but the lowest pressure case with $H/s_{\rm p} = 1$ yield unacceptable $\chi^2_{\rm red}$ values. Finally, *all* the cases with 10^5 photon counts (not shown) yield unacceptable 2-T model fits.

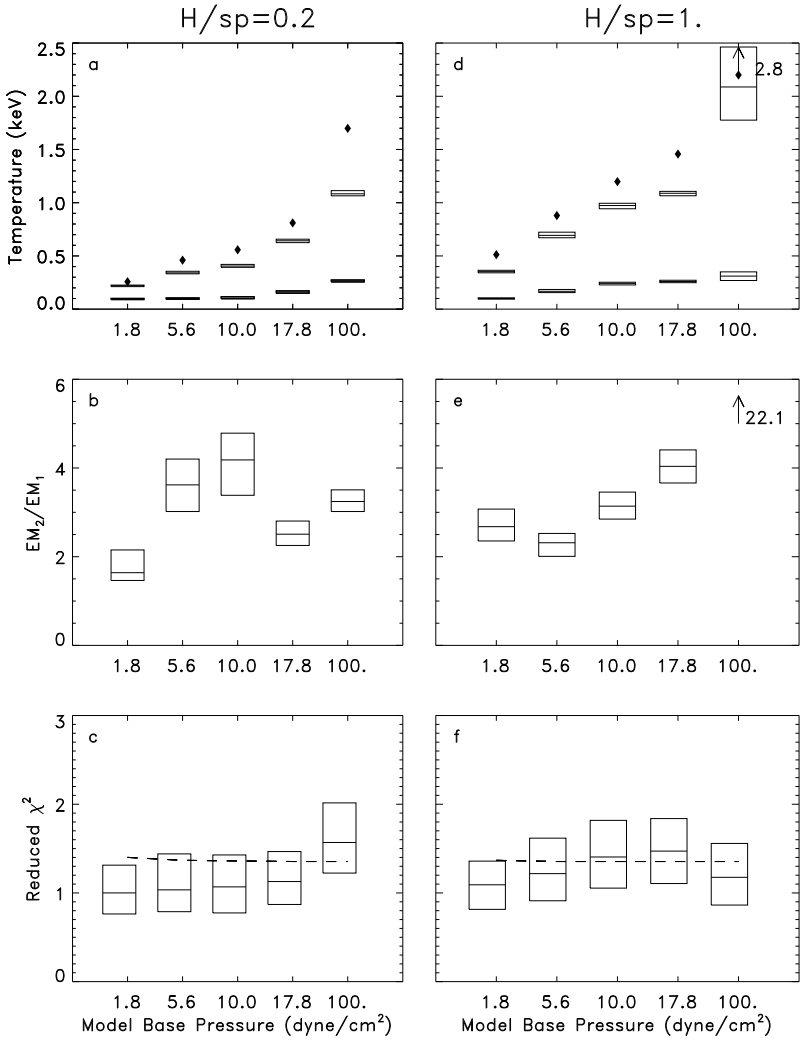

Fig. 6a–f. Fitting results for simulations of ROSAT/PSPC spectra of loops with expanding cross-section, assuming 10^4 total counts in each spectrum. The panels are arranged as in Fig. 4

Therefore, at variance with what found for the ROSAT/PSPC, even the 2-T model is in general an inadequate fitting tool for ASCA/SIS observations of coronae dominated by one kind of loop, most likely because the highest spectral resolution of ASCA/SIS permits to discriminate coronal loop spectra from a simple two-component thermal model. We expect that coronae containing even more than one kind of loops might yield even worse 2-T fittings because of the increasing complexity of the resulting spectrum.

3.3. Simulations with expanding loop geometries

In order to explore the effect of loop expansion on the fittings we have also considered a set of loops with quasi-radial expansion i.e., as assumed in Paper I, the cross sectional loop area varies with height above star's surface as:

$$S(s) = S_0(1 + h/R_*)^2 \quad (3)$$

For the loops with $H/s_{\rm p} = 0.2$ this amounts to an area expansion factor A_{top}/A_{base} ranging between 1.1 and 1.6 while for the loops with $H/s_{\rm p} = 1$, A_{top}/A_{base} ranges between 2.1 and 12.5.

A direct comparison with the analogous study of simulations without expansion shows that the loop expansion does not improve the 1-T fits significantly.

2-T fits, instead work at least equally well, i.e. they yield $\chi^2_{\rm red}$ values as in the simulations without expansion, or slightly smaller. The cooler fitted temperature is slightly higher than in the corresponding case without expansion reaching, at most 0.6 keV. The hotter temperature is definitely larger than in the case without expansion, especially for loops with $H/s_{\rm p} = 1$, and the emission measure of this component is much higher, especially for $H/s_{\rm p} = 1$ and the highest pressures.

In Fig. 6 we show, as an example, a set of simulations yielding 10^4 photons in ROSAT/PSPC, with $H/s_{\rm p} = 0.2$ and $H/s_{\rm p} = 1$, therefore amenable of direct comparison with the results of Fig. 4. Analogous results are found for the other cases with different counting statistics and for ASCA/SIS spectra, similar to those reported without expansion.

4. Discussion and conclusions

One of the purposes of the present work is to compare the 1-T and the 2-T models, generally used to fit the observed coronal spectra, with the modelling of stellar X-ray emission in terms

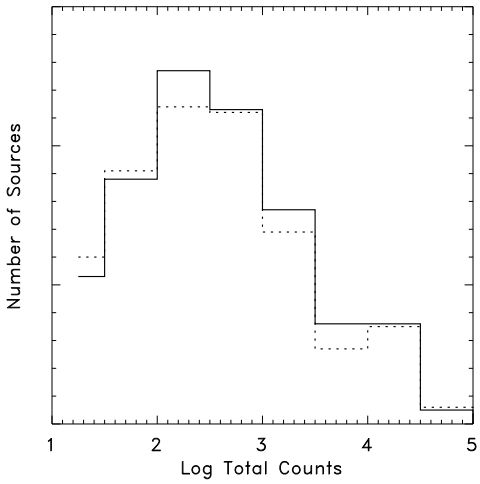

Fig. 7. Histograms of the number of X-ray sources in the MPE ROSAT/PSPC catalogue, matching the positions of late-type stars in the Catalogue of Nearby Stars (solid line) and in the Bright Star Catalogue (dotted line), vs. the total number of counts in their spectra. The linear y-axis range is from 0 to 150

of coronal loops. Another important aspect is to understand the insight that 1-T and 2-T fittings of real data can give on the characteristics of the loops present in the corona observed.

To this end we have devised and presented the 1-T and 2-T fittings of the loop spectra by generating spectra of stellar coronae entirely made with one kind of hydrostatic loops, and folded through the spectral response of ROSAT/PSPC and ASCA/SIS. This amounts to assume that the corona is largely dominated by a single class of loops.

We have concentrated our study on two levels of counting statistics (10^3 and 10^4 counts for the ROSAT/PSPC and 10^4 and 10^5 for the ASCA/SIS), typical of good or excellent observations, respectively, so as to show the information that can be achieved, at best, from the observations. In order to visualize how many stellar X-ray sources so far observed reach these counting statistics, Fig. 7 shows histograms of the number of X-ray sources in the MPE ROSAT/PSPC catalogue (Voges et al. 1995) identified[2] with late-type stars in the Catalogue of Nearby Stars (Gliese & Jahreiss 1991) and in the Bright Star Catalogue (Hoffleit & Warren 1991) vs. the number of counts in their spectra, computed from the listed count rates and exposure times.

The wide range of physical characteristics of loops used to model the coronae, allow us to obtain rather general conclusions. Our study shows that, in all the cases here considered, the 1-T fitting never gives acceptable results. The 2-T fits to coronal loop spectra of 10^3 total counts, collected with ROSAT/PSPC give, instead, acceptable results ($\chi^2_{\rm red} \approx 1$) in a wide range of conditions. However, for the highest pressure loops (with high plasma temperature: $T_{\rm max} \geq 10^7$ K) not even the 2-T fit works well with coronal loop PSPC spectra. It is worth noting that most published results of spectral analysis of real ROSAT/PSPC observations (e.g. Ottmann et al. 1993; Maggio et al. 1994b) show that a 1-T model usually does not yield acceptable fits of spectra with a high number of counts (and therefore high signal-to-noise) analogously to our results, at least hinting a scenario of coronae dominated by loops as observed on the Sun.

Coronal loop spectra of 10^4 counts collected with the ASCA/SIS can be fitted with two temperatures, and the results for coronal loop models with $H/s_{\rm p}$ = 0.2 at low pressure yield $\chi^2_{\rm red}$ values comparable to those determined with the ROSAT/PSPC with 10^3 counts; the ratio EM_2/EM_1 in this case is better defined. However, for higher pressures and maximum temperatures of the loops, the 2-T models are inadequate to fit coronal loop spectra. Furthermore, the goodness of the 2-T fitting is poor for any of the coronal loop spectra with 10^5 counts in the ASCA/SIS.

The spectral analysis of all the ASCA/SIS stellar spectra currently available (e.g. White et al. 1994; Drake et al. 1994; Singh et al. 1996) have been performed with 2-T models, and often a fitting of poor quality, from a statistical point of view, has been obtained if plasma solar abundances were assumed. In order to improve the goodness of the fit individual element abundances were set free to vary, and anomalous (i.e. non-solar) values were almost invariably obtained for the best 2-T model. In view of the present results it is worth asking whether assuming a (more realistic) loop model, instead of the 2-T model, would also lead to such anomalous abundances.

On the other hand, if one takes into account also some calibration uncertainties (Dotani et al. 1995), e.g. by adding systematic errors to the statistical ones, lower χ^2 values are derived, potentially bringing loop and 2-T fittings into better agreement, since the discrepancy between the two is not large in many cases. We have verified that assuming a uniform systematic error of 5% in each channel is sufficient to lower the χ^2 value of the fit reported in Fig. 1d (corresponding to the input loop spectrum κ) below the acceptance threshold (χ^2 = 233.5 for 207 d.o.f.). However, the issue of systematic errors is far from being definitive, and if instead the fitting could be taken as it is, then our simulations would prove that ASCA/SIS observations can discriminate between 2-T models and loops.

It appears that the spectrum of a loop, when observed with a good signal-to-noise level, can be fitted with two temperatures but never with a single temperature, at variance with the assumption – implicit in some studies (Schrijver et al. 1989; Giampapa et al. 1996) – that a loop yields a single temperature in the fitting. On the other hand it is easily conceivable (and some examples were shown in Paper I) that two dominant classes of loops may yield a spectrum, when observed with ROSAT/PSPC yielding good 2-T fits. Then the question is: when can one be sure to detect two classes of loops when two temperatures fit the spectrum ?

In this respect the EM_2/EM_1 ratio might provide important clues, since 2-T fittings of loops invariably yield $EM_2/EM_1 \gtrsim 1$. Fittings of real PSPC observations, instead, show a more complex scenario: in less active stars the ratio is usually $\lesssim 1$ (see, e.g., the old-disk M dwarfs studied by Micela et al. 1996 or the field F-type stars of Maggio et al. 1996), while on more active stars the ratio is often larger than 1 (e.g. most of the

[2] by requiring that angular positions in the sky match within 2 arcmin.

Hyades late-type dwarfs reported by Stern et al. 1994 or the F-G giants considered by Maggio et al. 1994b). Maybe a model with a single dominating kind of loops might work well with active stars and less well with non-active stars, although certainly it might appear strange that non-active stars require at least two classes of loops while active stars do not. However, Paper I has shown that even a small fraction of dense and hot loops may easily dominate a class of tenuous loops. On the other hand, some ROSAT observations yield $EM_2/EM_1 >> 1$ (e.g. many of the RS CVn - like systems studied by Dempsey et al. 1993 have $EM_2/EM_1 > 4$) or, more specifically, much larger than what obtained with the 2-T fits to the loops with constant cross section we have shown. In fact such loops give ratios, at most, around 4; loops with expansion, however, can give even much larger values of such a ratio. Therefore the observed large ratios could be explained in terms of a dominating class of loops with expansion but alternative explanations, which we do not explore here, cannot be excluded.

Our result contradicts the assumption that the observed coronae fitted with two-temperatures components are most probably dominated by two different classes of loops, each responsible for one fitted thermal component. Our results show that a corona dominated by only one class of loops could justify the 2-T components at 0.2 and 1.4 keV obtained in the fittings of the late-type stars (Schmitt et al 1990). It is worth noting, anyhow, that the fitted temperatures are never the same as the maximum loop plasma temperature, but rather they are indicative of a not straightforward weighting of the temperature distribution present in corona through the spectral response of the instrument.

The results of our study indicate that three factors play an important role in the interpretation of coronal loop spectra observed with PSPC and SIS: the number of collected counts, the spectral resolution and the coronal loop temperature. Even the 2-T fitting may become inappropriate for high number of counts (and therefore high statistical significance). On the other hand, the same coronal loop source, when observed at roughly equivalent signal-to-noise per channel with the PSPC and SIS, gives PSPC spectra which are well fitted with 2-T models and SIS spectra which instead are not adequately fitted. Finally, the fact that 2-T fits do not work for the highest pressure and maximum temperature loops may be explained by the increasing importance of the Fe L-shell complex at about 1 keV, that contains a number of lines belonging to a variety of ionization states (Fe XXVII - XXIV), corresponding to a wide range of temperatures (Mewe 1996, private communication).

Certainly the 2-T fitting is an easy tool to adopt for analyzing X-ray observations and it appears appropriate in deriving some effective (or average) coronal loop properties, however a correct interpretation of the analysis results should be done in the light of the present work. While 2-T fitting works reasonably well with real PSPC observations, it does not fare equally well with ASCA/SIS observations, and it is our contention that the reason has to be searched in the more physically complex coronal loop emission rather than in other exotic mechanisms.

Most likely, spectral fittings with loop models (Paper II shows a preliminary view in this perspective) should be used for future analysis of high signal-to-noise and/or high spectral resolution observations, as already evident in some of the present day observations, while we expect that spectra with few counts, e.g. 10^2 counts with ROSAT or 10^3 counts with ASCA/SIS, of non-flaring normal stars should be easily fitted with 2-T models.

Acknowledgements. We acknowledge useful comments and criticism from our colleagues S. Serio, F. Reale, F. Bocchino, and S. Sciortino. The authors also acknowledge partial support from Ministero dell'Universitá e della Ricerca Scientifica e Tecnologica, Agenzia Spaziale Italiana, and Gruppo Nazionale di Astronomia del Consiglio Nazionale delle Ricerche.

Appendix A: estimating the effective number of degrees of freedom

The χ^2 statistics[3] applies to the comparison between observed and expected binned data whose differences are asymptotically Gaussian distributed. Spectral bins with *few* counts do not conform to such a prescription and therefore they do not contribute properly to the χ^2, if included in the computation (see however the recent discussion of the problem by Wheaton et al. 1995). On the other hand, the correct minimum number of counts per bin granting a reliable χ^2 computation is not easily determined.

This problem plagues many X-ray observations, even of high S/N ratio, because the typical steep drop of the effective area of the X-ray instruments at high energies (due to the fall of reflectivity of the X-ray optics) together with the high energy cut-off of any thermal spectrum invariably yield few counts in the highest energy channels of the observed spectra.

In order to perform χ^2 fittings of such spectra, two alternative approaches are usually followed: (a) rebinning of the spectra with wider energy bins in order to achieve the required number of counts per bin, or (b) discarding the high energy bins with less than a given threshold number of counts. The former method suffers the drawback of having different binning schemes for different sources or even for different observations of the same source, implying that the comparison of distinct spectra is not straightforward. Moreover, the results of the fitting may be affected by the binning scheme, especially for detectors with relatively high spectral resolution, since the contribution of lines and continuous emission in each bin may depend on fine details of the spectral binning.

On the other hand, discarding bins with a number of counts below an adopted threshold saves the original binning, usually determined by a uniform oversampling of the spectral resolution vs. energy, and ensures uniformity of the spectral analysis throughout all the simulations; moreover, it is computationally simpler. For both these reasons we have adopted such a method. The approach for correcting the number of degrees of freedom

[3] $\chi^2 = \sum_j \frac{(o_j - e_j)^2}{\sigma_j^2}$, where o_j and e_j are, respectively, the observed and expected number of counts in each instrument energy bin, j, and $\sigma_j^2 \approx o_j$ is the variance of the data.

(henceforth d.o.f., nominally equal to the number of energy bins minus the number of free parameters), described below, has already been applied to the analysis of ROSAT/PSPC spectral fitting simulations with thermal models (Maggio et al. 1995); we refer to this work for further details.

Our rationale to find out the minimum number of counts per bin we want to keep, and hence the effective number of d.o.f. in the spectral analysis, is as follows: In performing the spectral fitting simulations, the null hypothesis is that the spectrum is drawn from the population represented by the predicted (model) spectrum. If we use the *same model* both to generate the simulated spectrum and to perform the subsequent fitting, this is certainly the case, and therefore we expect that the $\chi^2_{\rm red}$ distribution derived from a large number of realizations approaches the theoretical distribution for the nominal number of d.o.f. However, if some of the bins are empty (or nearly) they do not contribute properly to the χ^2 value, and therefore the $\chi^2_{\rm red}$ will be systematically underestimated because these bins do not carry enough information, leading to a $\chi^2_{\rm red}$ distribution significantly different from the theoretical one. In practice, we have checked that the χ^2 value does not change appreciably by discarding these bins, although the number of d.o.f. does change. Hence, by comparing simulated experimental distributions of $\chi^2_{\rm red}$ with the theoretical ones it is possible to estimate the effective number of d.o.f. which holds in the simulated spectral fittings.

More specifically, in Fig. 8 we compare theoretical and actual $\chi^2_{\rm red}$ distributions obtained from fitting 2-T simulated spectra (for a total of 200 realizations in each case) with 2-T models of a ROSAT/PSPC spectrum with 10^3 counts, and of an ASCA/SIS spectrum with 10^4 counts. In each case we show the two $\chi^2_{\rm red}$ distributions without any correction to the number of d.o.f. (left panels), and with the corrections which enforce agreement between the two distributions (right panels). We have verified that the effective number of d.o.f., derived in this way, is always less than the nominal number, and the difference is approximately equal to the number of energy bins with less than 0.5 counts per bin, in the parent (model) 2-T spectrum.

From these and other simulations of the same kind, we have drawn the following recipe to estimate the effective number of d.o.f. to be used in computing the $\chi^2_{\rm red}$ values of the spectral fitting simulations presented in this paper: for each simulation, first we generate the noiseless parent loop spectrum, and we count the number of energy bins with less than 0.5 counts per bin; then we perform the 2-T model fittings on the several (at least 200) realizations of the loop spectrum, properly including the Poisson noise, taking all bins into account; finally, we compute the $\chi^2_{\rm red}$ values adopting the effective number of d.o.f. which results from the nominal one after subtracting the bins with less than 0.5 counts each.

It is important to note that when we extend the recipe to 2-T fitting of simulated loop spectra, the parent spectrum of the simulated data and the model spectrum are different, and we cannot expect that the actual $\chi^2_{\rm red}$ distribution overlaps with the theoretical one. Nevertheless, for the loop spectra which turn out to be well approximated by 2-T models, we have verified – a posteriori – that the correction ensures a reasonable overlap between the two distributions. This agreement cannot be expected, of course, when fitting loop spectra with shapes significantly different from the shape of 2-T models. If no correction to the number of d.o.f. is taken into account, even blatant discrepancies between simulated data and model spectrum do not lead to high *reduced* χ^2 values because the nominal number of d.o.f. overestimates the "effective" value.

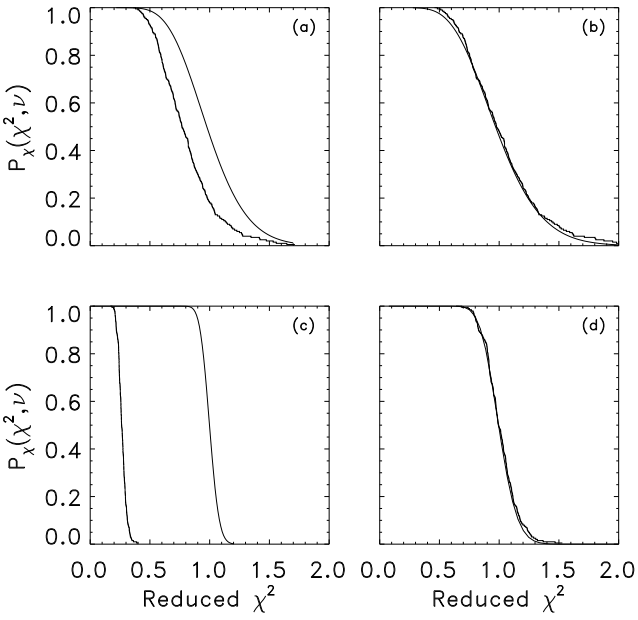

Fig. 8a–d. Comparison of theoretical and actual reduced χ^2 distributions. **a** Spectral fitting simulation for a 2-T ROSAT/PSPC spectrum with 10^3 counts, having T_1 = 0.10 keV, T_2 = 0.34 keV, EM_2/EM_1 = 3.2, for the nominal number of d.o.f = 28; the theoretical distribution is the smooth curve on the right. **b** Same simulation but assuming 22 d.o.f., which yields the best overlap between the two $\chi^2_{\rm red}$ distributions. **c** Simulation for a 10^4 counts ASCA/SIS spectrum with T_1 = 0.4 keV, T_2 = 1.0 keV, EM_2/EM_1 = 1.1, and assuming 495 d.o.f. (nominal number). **d** Same simulation but assuming 131 d.o.f., to achieve the best overlap

References

Ciaravella A., Peres G., Maggio A., Serio S., 1996, A&A 306, 553 (Paper I)

Dempsey R.C., Linsky J.L., Schmitt J.H.M.M., Fleming T.A., 1993, ApJ 413, 333

Dotani T., Yamashita A., Rasmussen A., 1995, ASCA News No. 3

Drake S., Singh K., White N., Simon T., 1994, ApJ 436, L87.

Eadie W.T., Drijard D., James F.E., Roos M., Sadoulet B., 1982, Statistical Methods in Experimental Physics, North-Holland Pub. Comp.

Giampapa M.S., Golub L., Peres G., Serio S., Vaiana G.S., 1985, ApJ 289, 203

Giampapa M.S., Rosner R., Kashyap V., Fleming T.A., Schmitt J.H.M.M., 1996, ApJ 463, 707

Gliese W., Jahreiss H., 1991, Catalogue of Nearby Stars, 3rd edition (Preliminary version, available at CDS and GSFC public data archives)

Hoflleit D., Warren W.H. Jr., 1991, Bright Star Catalogue, 5th revised edition (Preliminary version, available at CDS and GSFC public data archives)
Landini M., Monsignori Fossi B.C., Paresce F., Stern R.A., 1985, ApJ 289, 709
Lemen J.R., Mewe R., Schrijver C.J., Fludra, 1989, ApJ 341, 474
Maggio A., Peres G., 1996, A&A 306, 563 (Paper II)
Maggio A., Peres G., Reale F., Ciaravella A., 1994a, CPC 81, 105
Maggio A., Sciortino S., Harnden F.R. Jr., 1994b, ApJ 432, 701
Maggio A., Sciortino S., Collura A., Harnden F.R. Jr., 1995, A&AS 110, 573
Maggio A., Peres G., Pye J.P., Hodgkin J.E., Morley J.E., 1996, Proceedings of 9th Cambridge Workshop on Cool Stars, Stellar Systems and the Sun, in press
Micela G., Pye J.P., Sciortino S., 1996, A&A, submitted
Ottmann R., 1993, A&A, 273, 546
Ottmann R., Schmitt J.H.M.M., Kuerster M., 1993, ApJ, 413, 710
Rosner R., Tucker W.H., Vaiana G.S., 1978, ApJ 220, 643
Rosner R., Golub W., Vaiana G.S., 1985, ARAA 23, 413
Schmitt J.H.M.M., Harnden F.R., Peres G., Rosner R., Serio S., 1985, ApJ 288, 751
Schmitt J., Collura A., Sciortino S., et al., 1990, ApJ 365, 704
Schrijver C.J., Lemen J.R., Mewe R., 1989, ApJ 341, 484
Serio S., Peres G., Vaiana G.S., Golub L., Rosner, R., 1981, ApJ 243, 288
Singh K., Drake S., White N., 1995, ApJ 457, 598
Stern R.A, Antiochos S., Harnden F.R., 1986, ApJ 305, 417
Stern R.A., Schmitt J.H.M.M., Pye J.P., Hodgkin S.T., Stauffer J.R., 1994, ApJ 427, 808
Raymond J., 1989, private communication
Vaiana G.S. et al., 1981, ApJ 245, 163
Voges W., Gruber R., Haberl F., et al., 1994, ROSAT News No. 32
Wheaton Wm. A., Dunklee A.L., Jacobson A.S., et al., 1995, ApJ 438, 322
White N. et al., 1994, PASJ 46, L97

This article was processed by the author using Springer-Verlag LaTeX A&A style file *L-AA* version 3.